JACS
JOURNAL OF THE AMERICAN CHEMICAL SOCIETY
Communication
pubs.acs.org/JACS

Direct Observation of the Hole Carriers in DNA Photoinduced Charge Transport

Michelle A. Harris, Ashutosh Kumar Mishra, Ryan M. Young, Kristen E. Brown, Michael R. Wasielewski,* and Frederick D. Lewis*

Department of Chemistry and Argonne-Northwestern Solar Energy Research (ANSER) Center, Northwestern University, Evanston, Illinois 60208-3113, United States

Supporting Information

ABSTRACT: The excited state behavior of DNA hairpins possessing a diphenylacetylenedicarboxamide (DPA) linker separated from a single guanine−cytosine (G−C) base pair by zero-to-six adenine−thymine (A−T) base pairs has been investigated. In the case of hairpins with zero or one A−T separating DPA and G, formation of both DPA anion radical ($DPA^{-\bullet}$) and G cation radical ($G^{+\bullet}$) are directly observed and characterized by their transient absorption and stimulated Raman spectra. For hairpins with two or more intervening A−T, the transient absorption spectra of $DPA^{-\bullet}$ and the adenine polaron ($A_n^{+\bullet}$) are observed. In addition to characterization of the hole carriers, the dynamics of each step in the charge separation and charge recombination process as well as the overall efficiency of charge separation have been determined, thus providing a complete account of the mechanism and dynamics of photoinduced charge transport in these DNA hairpins.

The mechanism of photoinduced charge separation in DNA has been the subject of active investigation for over two decades.[1] Charge separation was initially thought to occur via a single-step tunneling mechanism in which charge never resides on the base pairs separating the electron donor and acceptor;[2] however, tunneling is now thought to occur only in cases where charge injection from an excited chromophore into the adjacent base is highly endergonic.[3,4] When charge injection is moderately endergonic or exergonic, charge separation occurs via the initial formation of an exciplex or radical ion pair between the excited chromophore and an adjacent base.[5,6] The transport of positive charge from the adjacent base to a distal hole trap has been proposed to occur via several different mechanisms including the single-step tunneling[7] and flickering resonance[8] mechanisms, incoherent hopping in which the positive charge is localized on a single base,[9] and polaron-like transport in which the hole is delocalized over several bases.[10−13]

Guanine (G) is the most readily oxidized of the four common bases and has been employed both as a hole trap in studies of photoinduced charge separation[14] and as an intermediate in long-distance, multistep charge transport processes.[15] The G cation radical, $G^{+\bullet}$, is also the putative initial intermediate in the oxidative cleavage of DNA.[16] Thus, there have been numerous studies of the formation and behavior of $G^{+\bullet}$ both as the nucleotide and in single strand and duplex DNA. Absorption spectroscopy,[17−19] EPR,[19] and vibrational spectroscopy[20] have been employed to detect and characterize $G^{+\bullet}$. Zinth and co-workers have recently reported the characterization of $G^{+\bullet}$ by transient infrared spectroscopy following femtosecond laser excitation of G-containing dinucleotides,[21] thus suggesting the potential of vibrational spectroscopy for detecting the formation of $G^{+\bullet}$ as a short-lived intermediate within duplex DNA.

We report here the results of an investigation of photoinduced charge transport in DPA−A_nG hairpins (Chart 1), where DPA is the hole donor diphenylacetylenedicarboxamide. A combination of femtosecond and nanosecond transient absorption spectroscopy (fsTA and nsTA, respectively) and femtosecond stimulated Raman spectroscopy (FSRS) has been employed to characterize the DPA anion radical ($DPA^{-\bullet}$), the guanine cation radical ($G^{+\bullet}$), and the adenine polaron ($A_n^{+\bullet}$) intermediates in the charge transport process (Scheme 1). DPA was selected for this study on the basis of the relatively narrow and well-resolved transient absorption bands for its singlet and anion radical[22,23] and its high quantum yield of charge separation in DNA hairpins,[24] which together allow for observation and analysis of charge separation and the resulting intermediates.

Chart 1. Structures of the DPA Diol Linker and the DPA-Linked Hairpins

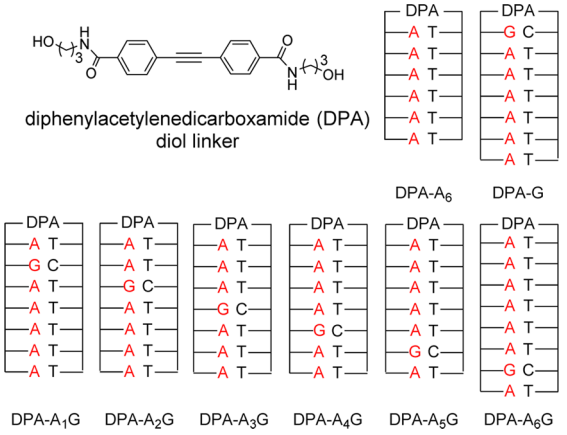

The DPA-linked hairpins (Chart 1) were prepared and characterized as previously reported (see Supporting Information).[22,23] Their UV spectra consist of a band with two vibronic

Received: January 20, 2016
Published: April 15, 2016

DOI: 10.1021/jacs.6b00702
J. Am. Chem. Soc. 2016, 138, 5491−5494

Scheme 1. Mechanism for Photoinduced Hole Injection from ^{1}*DPA to (a) an Adjacent G and to (b) an A_n Tract Followed by Hole Transport to G and Charge Recombination from $(A_n)^{+\bullet}$ or $G^{+\bullet}$[a]

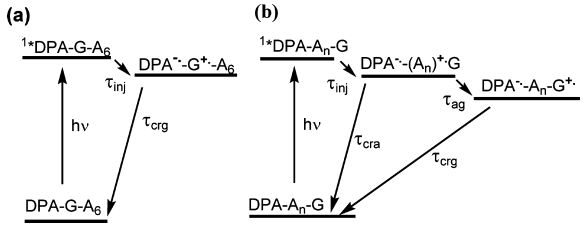

[a]Hairpin DPA-A_6 is similar to hairpin DPA-A_6G except for lacking the terminal G.

maxima between 300 and 350 nm assigned to the DPA chromophore and a broad band at 260 nm assigned to overlapping absorption of the DNA bases and DPA. DPA-linked hairpins are very weakly fluorescent ($\Phi_f < 10^{-4}$) indicative of efficient fluorescence quenching of the DPA chromophore by either an A−T or G−C adjacent base pair.[23] The CD spectrum of a DPA-linked hairpin having five A−T base pairs is similar to that of poly(dA)·poly(dT) indicative of the formation of a B-DNA base pair domain.[23]

The excited-state behavior of limited sets of DPA-linked hairpins has previously been investigated by our group using fsTA[23] and by Takada et al. using nsTA.[24] We have now studied a complete set of DPA−A_nG (n = 0−6) hairpins using fsTA, nsTA, and FSRS. The fsTA and nsTA spectra of the DPA hairpins at selected times following laser excitation are shown in Figure 1. In

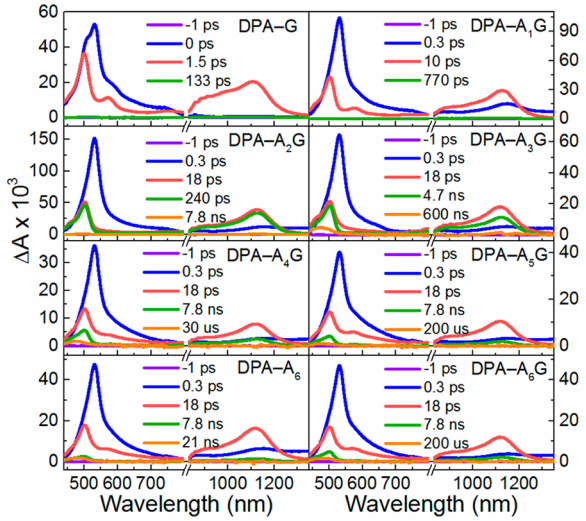

Figure 1. FsTA and nsTA spectra for the hairpins in Chart 1 at the indicated delay times following a 330 nm laser pump pulse in aqueous buffer. The nsTA spectra shown (>8 ns) were scaled to fsTA when necessary by comparing the 7 ns spectra.

all cases, a single band at 525 nm is formed within the ca. 150 fs instrument response using a 330 nm laser pump pulse, decays within several ps, and is replaced by a sharp band at 500 nm (ca. 30 nm fwhm, Table S2) and a broad band at 1130 nm in the near-infrared (NIR) region. The 525 and 500 nm bands are assigned to ^{1}*DPA and $DPA^{-\bullet}$, respectively, as in our earlier investigation.[23] The NIR band was not observed previously due to limited detection range. Its assignment to $DPA^{-\bullet}$ is consistent with the kinetics of its formation and decay, which follow those of the 500 nm band. The UV and NIR bands for $DPA^{-\bullet}$ are similar in shape, but are blue-shifted with respect to those for the unsubstituted $DPA^{-\bullet}$ in a MTHF glass as reported by Shida.[25] The distinct spectral features of $DPA^{-\bullet}$ provide convenient markers for tracking the dynamics of its formation and decay.

Global analysis of the transient absorption spectra provides the rise times for $DPA^{-\bullet}$ formation, which are attributed to hole injection to the neighboring G or A bases (τ_{inj}, Scheme 1a,b; see Supporting Information Figures S1−S14 for global fitting and modified global fitting and species associated spectra for the hairpins in Chart 1). The τ_{inj} values reported in Table 1 are

Table 1. Properties of DPA Hairpin Intermediates[a]

hairpin	τ_{inj} (ps)	τ_a (ns)	τ_{cra} (ns)	τ_{ag} (ns)	τ_{crg} (ns)	Φ_g
DPA−A_6	2.8	2.5	2.5			0.0
DPA−G	0.26				0.022	1.0
DPA−A_1G	1.6				0.13[b]	1.0
DPA−A_2G	2.6	0.034	0.25[c]	0.045[c]	1.8	0.85
DPA−A_3G	2.6	0.79	2.0[c]	1.3[c]	100	0.61
DPA−A_4G	3.0	1.5	2.1[c]	4.9[c]	5100	0.30
DPA−A_5G	3.1	1.5	2.1[c]	5.4[c]	27,000	0.28
DPA−A_6G	2.7	1.5	2.1[c]	5.4[c]	55,000	0.28

[a]See Supporting Information for analytical methods. [b]$\tau_{ag} \ll \tau_{cra}$ for DPA-A1G. [c]Calculated from τ_a and Φ_g.

smaller for DPA−G and DPA−A_1G (0.25 and 1.6 ps, respectively) than for hairpins having two or more A bases adjacent to DPA (2.6−3.1 ps). Values of τ_{inj} are in good agreement with those previously reported for several DPA hairpins.[23]

In addition to the formation of the transient absorption bands for $DPA^{-\bullet}$, which are observed for all of the hairpins, a weaker but distinct band is observed at 575 nm in the transient spectra of DPA−G and DPA−A_1G (Figure 1), but none of the other hairpins. This band tracks the formation and decay of $DPA^{-\bullet}$. Decay of both bands is attributed to charge recombination of $DPA^{-\bullet}$−$G^{+\bullet}$ and $DPA^{-\bullet}$−$A_1G^{+\bullet}$ (τ_{crg}, Scheme 1a,b (n = 1) and Table 1).

Support for the assignment of the 575 nm band to $G^{+\bullet}$ is provided by the FSRS spectra obtained using a 575 nm Raman pump pulse following 330 nm actinic excitation as shown in Figure 2. The spectra of hairpins DPA−G and DPA−A_1G, but

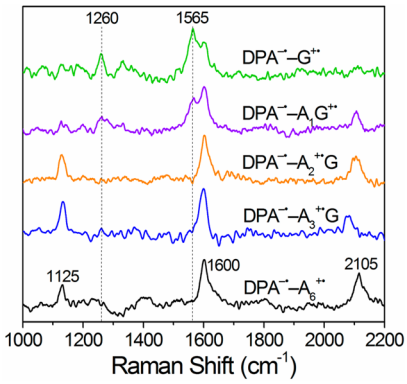

Figure 2. Normalized femtosecond stimulated Raman spectra, obtained using a 575 nm Raman pump following 330 nm actinic excitation, of the hairpins at a time point ca. 6 × τ_{inj}. The peaks are labeled accordingly, and the major $G^{+\bullet}$ features are denoted with vertical dashed lines.

DOI: 10.1021/jacs.6b00702
J. Am. Chem. Soc. 2016, 138, 5491−5494

not DPA−A_2G, DPA−A_3G, or DPA−A_6, display bands at 1260 and 1565 cm^{-1} assigned to $G^{+\bullet}$ (Figures 2 and S15−S23). The Raman features assigned to $G^{+\bullet}$ are similar to those previously reported for a G-containing triad.[26] Our observed features are similar but shifted from those recently calculated by Sevilla et al. for $G^{+\bullet}$ in the guanine base and nucleotide.[27] These shifts plausibly reflect base pairing and ion pairing. The rise and decay times of the $G^{+\bullet}$ Raman bands are similar to those for the 575 nm band in the fsTA spectra (Figures S1, S2, S16, and S18). The Raman spectra of all of the hairpins studied display bands at 1125, 1600, and 2105 cm^{-1} assigned to $DPA^{-\bullet}$ (Figures 2 and S15−S23). The Raman signature assigned to $DPA^{-\bullet}$ matches a previous time-resolved resonance Raman spectrum reported by Hiura et al.[28]

The 575 nm transient absorption band assigned to $G^{+\bullet}$ is red-shifted and narrower than the weak 500 nm absorption bands reported by previous workers using pulse radiolysis-transient absorption with much slower time resolution.[17] A weak 500 nm band most likely would not have been detected in the presence of the strong $DPA^{-\bullet}$ band. Hairpins possessing two or more adenines adjacent to DPA fail to display the 1260 or 1565 cm^{-1} bands in FSRS assigned to $G^{+\bullet}$, at all decay times (Figures 2 and S15−S23). A plausible explanation for the absence of these marker bands for hairpins with $n \geq 2$ is provided by charge delocalization of $G^{+\bullet}$ with its neighboring adenines. According to the wave functions for single strand poly-A oligomers containing a single $G^{+\bullet}$ calculated by Conwell and co-workers, the positive charge on $G^{+\bullet}$ is partially delocalized onto the adjacent As, in what Conwell refers to as a G-polaron.[29] While the time scale for $G^{+\bullet}$ charge delocalization is not known, the structural relaxation that determines the internal reorganization energy for charge delocalization might require times longer than the 130 ps charge recombination time for $DPA^{-\bullet}$−$A_1G^{+\bullet}$. The time constant for charge transport in a G-tract is ca. 200 ps/base.[30] Increased charge delocalization would result in broadening and decreased intensity of the $G^{+\bullet}$ marker bands. Rapid reversible $G^{+\bullet}$−C proton transfer[18,31] provides an alternative explanation for the absence of the $G^{+\bullet}$ marker bands. However, the dynamics and mechanism of $G^{+\bullet}$ deprotonation and reprotonation remain subjects of controversy.[32]

The DPA−A_nG hairpins with $n \geq 2$ do not display 1260 and 1565 cm^{-1} FSRS bands, yet they do show 565 nm fsTA bands, which increase in intensity with the number of As, attaining a maximum intensity in the normalized transient absorption spectrum of DPA−A_5G (Figure 3). The 565 nm bands in the transient absorption spectra are assigned to an A-polaron delocalized over the first 2−4 adenines with the positive charge skewed toward the negative charge on $DPA^{-\bullet}$ by Coulombic attraction. This feature is broader than the absorption band assigned to $G^{+\bullet}$ (fwhm = 161 ± 16 nm vs 41 ± 2 nm, Table S2) and is also present in the spectrum of DPA−A_6. The greater bandwidth is consistent with greater delocalization in an $A_n^{+\bullet}$ vs $AGA^{+\bullet}$.[11,33] The 565 nm feature decays well before $DPA^{-\bullet}$ in DPA−A_nG with $n \geq 2$, indicating that it is not associated with charge recombination from $DPA^{-\bullet}$−$A_nG^{+\bullet}$ in these hairpins. The lifetime of $A_n^{+\bullet}$ (τ_a) increases with n from 34 ps for DPA−A_2G to 1.5 ns for DPA−A_{4-6}G (Table 1). The Raman spectra of hairpins DPA−A_2G, DPA−A_3G, and DPA−A_6 (Figures 2 and S15−S23) exhibit only $DPA^{-\bullet}$ features confirming that the 565 nm band is not a $G^{+\bullet}$ signature. The absence of Raman bands associated with the A-polaron is not surprising as stacking of chromophores can lead to frequency shifts and loss of intensity both for neutrals and polarons.[34]

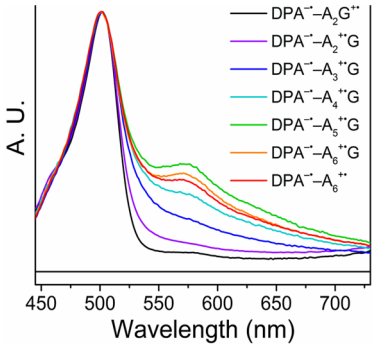

Figure 3. Normalized fsTA spectra for the hairpins that show the broad A-polaron feature around 565 nm. The spectra are at a time point immediately after complete charge injection ($6 \times \tau_{inj}$, ca. 18 ps) except for the indicated reference spectrum of $DPA^{-\bullet}$−$A_2G^{+\bullet}$ (black trace) showing hole arrival on G at 240 ps.

Recent theoretical analysis of photoinduced charge transport in stilbenedicarboxamide-linked hairpins by Renaud et al. have predicted the formation of precisely this type of polaron.[13] We previously suggested that a polaron rather than hole hopping was responsible for hole transport from singlet perylenediimide (PDI) to G following hole injection to A_n (n = 2−4) in PDI−A_nG hairpins.[12] It is interesting to note that the number of A−T base pairs required for the maximum lifetime and intensity for the A-polaron, four A−T base pairs, is the same as that required for the structural features characteristic of A-tract DNA (e.g., narrow minor groove and characteristic hydration motifs).[35]

The shorter lifetime for the polaron than for $DPA^{-\bullet}$ suggests that the polaron can decay both by charge recombination with $DPA^{-\bullet}$ and by hole transport to G (τ_{cra} and τ_{ag}, Scheme 1b). The efficiency of hole transport to G (Φ_G, Table 1) decreases as the number of intervening As increases and levels off after four As; as seen in other DNA hairpins.[36] The yields are higher than those reported by Takada et al. based on nsTA measurements for DPA-linked hairpins, but corroborate their conclusion that charge separation is uncommonly efficient in these hairpins.[24] The constant values of Φ_g for DPA−A_nG hairpins with $n \geq 4$ would seemingly preclude charge transport mechanisms involving tunneling or incoherent hopping from the contact ion pair. Decay times for charge recombination of $A_n^{+\bullet}$ (τ_{cra}) and hole transport to G (τ_{ag}) can be calculated from the measured values of Φ_g, the effective lifetime of $A_n^{+\bullet}$ (τ_a), and the relationship $\Phi_g = k_{ag}/k_a$ ($k_a = k_{cra} + k_{ag}$ and $k = 1/\tau$). The resulting values of τ_{cra} and τ_{ag} are reported in Table 1. The value of τ_{cra} is shorter for DPA−A_2G than for the other hairpins (0.25 vs 2−2.5 ns); whereas the values of τ_{ag} increase more gradually with the spatial extent of the polaron, as previously observed for the PDI hairpins.[12]

Values of τ_{crg}, the charge recombination times for the $DPA^{-\bullet}$−$A_nG^{+\bullet}$ charge separated states, can be determined from the decay of the $DPA^{-\bullet}$ bands in their fsTA or nsTA spectra. In the case of DPA−G and DPA−A_1G, the decay kinetics of the 575 nm $G^{+\bullet}$ bands and the $DPA^{-\bullet}$ bands are the same. Values of τ_{crg} are reported in Table 1 and are seen to increase exponentially with the length of the A-tract from DPA−G (22 ps) to DPA−A_4G (5.1 μs), but increase more slowly at longer distances. This biphasic distance dependence is similar to that previously reported for stilbenedicarboxamide-linked hairpins.[37] There is a minor contribution at 485 nm with a lifetime >100 μs in DPA−A_nG with $n \geq 3$, which we identify as ^{3}*DPA (see Figures S6, S8, S10, S12, and S14).

DOI: 10.1021/jacs.6b00702
J. Am. Chem. Soc. 2016, 138, 5491−5494

In summary, the distinct bands of the ^{1}*DPA and DPA$^{-\bullet}$ transient absorption spectra permit tracking the hole injection process in the DPA hairpins while leaving the spectral window needed for observation of the G$^{+\bullet}$ and A$_n^{+\bullet}$ intermediates in the charge transport process unobscured. The formation of G$^{+\bullet}$ within a DNA duplex by means of photoinduced charge separation has been observed for the first time by visible fsTA spectroscopy and FSRS. Of equal significance to understanding the mechanism of charge transport in DNA is the observation of the A$_n^{+\bullet}$ by means of fsTA spectroscopy. This observation would seem to resolve the long-standing uncertainty concerning the mechanism of hole transport following charge injection into DNA. While polarons have been frequently invoked as intermediates in DNA charge transport processes,[10,38] there has been no prior report of their spectroscopic observation. The A$_n^{+\bullet}$ observed here is formed adjacent to DPA$^{-\bullet}$ where hole injection occurs. However, the similar values of τ_{ag} and Φ_g for DPA−A$_n$G where n = 4−6 suggest that these polarons are not constrained to the first few base pairs. We caution that the behavior of the polaron may well be dependent upon the energetics of its formation and trapping as well as the length of the A-tract. Continued experimental and theoretical studies of photoinduced charge transport processes are in progress.

■ ASSOCIATED CONTENT

Supporting Information

The Supporting Information is available free of charge on the ACS Publications website at DOI: 10.1021/jacs.6b00702.

Hairpin synthesis and mass spectral data; nanosecond and femtosecond transient absorption spectra and data analysis; femtosecond stimulated Raman spectra and data analysis (PDF)

■ AUTHOR INFORMATION

Corresponding Authors

*m-wasielewski@northwestern.edu
*fdl@northwestern.edu

Notes

The authors declare no competing financial interest.

■ ACKNOWLEDGMENTS

This research was funded by the Office of Naval Research MURI grant no. N00014-11-1-0729.

■ REFERENCES

(1) (a) Genereux, J. C.; Barton, J. K. *Chem. Rev.* **2010**, *110*, 1642. (b) Kawai, K.; Majima, T. *Acc. Chem. Res.* **2013**, *46*, 2616. (c) Lewis, F. D. *Isr. J. Chem.* **2013**, *53*, 350.

(2) Lewis, F. D.; Wu, T.; Zhang, Y.; Letsinger, R. L.; Greenfield, S. R.; Wasielewski, M. R. *Science* **1997**, *277*, 673.

(3) Lewis, F. D.; Liu, J.; Weigel, W.; Rettig, W.; Kurnikov, I. V.; Beratan, D. N. *Proc. Natl. Acad. Sci. U. S. A.* **2002**, *99*, 12536.

(4) Lewis, F. D.; Zhang, L.; Kelley, R. F.; McCamant, D.; Wasielewski, M. R. *Tetrahedron* **2007**, *63*, 3457.

(5) Lewis, F. D.; Zhu, H.; Daublain, P.; Fiebig, T.; Raytchev, M.; Wang, Q.; Shafirovich, V. *J. Am. Chem. Soc.* **2006**, *128*, 791.

(6) Singh, A. P. N.; Harris, M. A.; Young, R. M.; Miller, S. A.; Wasielewski, M. R.; Lewis, F. D. *Faraday Discuss.* **2015**, *185*, 105.

(7) Blaustein, G. S.; Lewis, F. D.; Burin, A. L. *J. Phys. Chem. B* **2010**, *114*, 6732.

(8) Zhang, Y.; Liu, C.; Balaeff, A.; Skourtis, S. S.; Beratan, D. N. *Proc. Natl. Acad. Sci. U. S. A.* **2014**, *111*, 10049.

(9) (a) Jortner, J.; Bixon, M.; Langenbacher, T.; Michel-Beyerle, M. E. *Proc. Natl. Acad. Sci. U. S. A.* **1998**, *95*, 12759. (b) Meggers, E.; Michel-Beyerle, M. E.; Giese, B. *J. Am. Chem. Soc.* **1998**, *120*, 12950.

(10) Henderson, P. T.; Johes, D.; Hampikian, G.; Kan, Y.; Schuster, G. B. *Proc. Natl. Acad. Sci. U. S. A.* **1999**, *96*, 8353.

(11) Conwell, E. M.; Bloch, S. M.; McLaughlin, P. M.; Basko, D. M. *J. Am. Chem. Soc.* **2007**, *129*, 9175.

(12) Zeidan, T. A.; Carmieli, R.; Kelley, R. F.; Wilson, T. M.; Lewis, F. D.; Wasielewski, M. R. *J. Am. Chem. Soc.* **2008**, *130*, 13945.

(13) Renaud, N.; Berlin, Y. A.; Lewis, F. D.; Ratner, M. A. *J. Am. Chem. Soc.* **2013**, *135*, 3953.

(14) (a) Lewis, F. D.; Wu, T.; Liu, X.; Letsinger, R. L.; Greenfield, S. R.; Miller, S. E.; Wasielewski, M. R. *J. Am. Chem. Soc.* **2000**, *122*, 2889. (b) Wan, C.; Fiebig, T.; Schiemann, O.; Barton, J. K.; Zewail, A. H. *Proc. Natl. Acad. Sci. U. S. A.* **2000**, *97*, 14052.

(15) (a) Schuster, G. B. *Acc. Chem. Res.* **2000**, *33*, 253. (b) Giese, B. *Acc. Chem. Res.* **2000**, *33*, 631.

(16) Yun, B. H.; Lee, Y. A.; Kim, S. K.; Kuzmin, V.; Kolbanovskiy, A.; Dedon, P. C.; Geacintov, N. E.; Shafirovich, V. *J. Am. Chem. Soc.* **2007**, *129*, 9321.

(17) Kobayashi, K.; Tagawa, S. *J. Am. Chem. Soc.* **2003**, *125*, 10213. Candeias, L. P.; Steenken, S. *J. Am. Chem. Soc.* **1989**, *111*, 1094.

(18) Kobayashi, K.; Yamagami, R.; Tagawa, S. *J. Phys. Chem. B* **2008**, *112*, 10752.

(19) Adhikary, A.; Kumar, A.; Becker, D.; Sevilla, M. D. *J. Phys. Chem. B* **2006**, *110*, 24171.

(20) Parker, A. W.; Lin, C. Y.; George, M. W.; Towrie, M.; Kuimova, M. K. *J. Phys. Chem. B* **2010**, *114*, 3660.

(21) Bucher, D. B.; Pilles, B. M.; Carell, T.; Zinth, W. *Proc. Natl. Acad. Sci. U. S. A.* **2014**, *111*, 4369.

(22) Lewis, F. D.; Liu, X.; Miller, S. E.; Wasielewski, M. R. *J. Am. Chem. Soc.* **1999**, *121*, 9746.

(23) Lewis, F. D.; Liu, X.; Miller, S. E.; Hayes, R. T.; Wasielewski, M. R. *J. Am. Chem. Soc.* **2002**, *124*, 14020.

(24) Takada, T.; Kawai, K.; Fujitsuka, M.; Majima, T. *Angew. Chem., Int. Ed.* **2006**, *45*, 120.

(25) Shida, T. *Electronic Absorption Spectra of Radical Ions*; Elsevier: Amsterdam, 1988.

(26) Wu, Y.-L.; Brown, K. E.; Gardner, D. M.; Dyar, S. M.; Wasielewski, M. R. *J. Am. Chem. Soc.* **2015**, *137*, 3981.

(27) Sevilla, M. D.; Kumar, A.; Adhikary, A. *J. Phys. Chem. B* **2016**, *120*, 2984.

(28) Hiura, H.; Takahashi, H. *J. Phys. Chem.* **1992**, *96*, 8909.

(29) Kucherov, V. M.; Kinz-Thompson, C. D.; Conwell, E. M. *J. Phys. Chem. C* **2010**, *114*, 1663.

(30) Mickley Conron, S. M.; Thazhathveetil, A. K.; Wasielewski, M. R.; Burin, A. L.; Lewis, F. D. *J. Am. Chem. Soc.* **2010**, *132*, 14388.

(31) Steenken, S. *Biol. Chem.* **1997**, *378*, 1293.

(32) (a) Kawai, K.; Osakada, Y.; Majima, T. *ChemPhysChem* **2009**, *10*, 1766. (b) Choi, J.; Yang, C.; Fujitsuka, M.; Tojo, S.; Ihee, H.; Majima, T. *J. Phys. Chem. Lett.* **2015**, *6*, 5045.

(33) Kumar, A.; Sevilla, M. D. *J. Phys. Chem. B* **2011**, *115*, 4990.

(34) (a) Milani, A.; Brambilla, L.; Del Zoppo, M.; Zerbi, G. *J. Phys. Chem. B* **2007**, *111*, 1271. (b) Magnanelli, T. J.; Bragg, A. E. *J. Phys. Chem. Lett.* **2015**, *6*, 438.

(35) (a) Han, G. W.; Kopka, M. L.; Cascio, D.; Grzeskowiak, K.; Dickerson, R. E. *J. Mol. Biol.* **1997**, *269*, 811. (b) Woods, K. K.; Maehigashi, T.; Howerton, S. B.; Sines, C. C.; Tannenbaum, S.; Williams, L. D. *J. Am. Chem. Soc.* **2004**, *126*, 15330.

(36) Lewis, F. D.; Zhu, H.; Daublain, P.; Cohen, B.; Wasielewski, M. R. *Angew. Chem., Int. Ed.* **2006**, *45*, 7982.

(37) Lewis, F. D.; Zhu, H.; Daublain, P.; Sigmund, K.; Fiebig, T.; Raytchev, M.; Wang, Q.; Shafirovich, V. *Photochem. Photobiol. Sci.* **2008**, *7*, 534.

(38) (a) Schuster, G. B.; Landman, U. *Top. Curr. Chem.* **2004**, *236*, 139. Conwell, E. M.; Rakhmanova, S. V. *Proc. Natl. Acad. Sci. U. S. A.* **2000**, *97*, 4556. (b) Conwell, E. M. *Proc. Natl. Acad. Sci. U. S. A.* **2005**, *102*, 8795.

DOI: 10.1021/jacs.6b00702
J. Am. Chem. Soc. 2016, 138, 5491−5494